# Addition of Small Electrophiles to N-Heterocyclic-Carbene-Stabilized Disilicon(0): A Revisit of the Isolobal Concept in Low-Valent Silicon Chemistry

Marius I. Arz, Martin Straßmann, Daniel Geiß, Gregor Schnakenburg, and Alexander C. Filippou*

Institute of Inorganic Chemistry, University of Bonn, Gerhard-Domagk-Straße 1, D-53121 Bonn, Germany

S *Supporting Information*

ABSTRACT: Protonation and alkylation of (Idipp)Si=Si-(Idipp) (**1**) afforded the mixed-valent disilicon(I)-borates $[(Idipp)(R)Si^{II}=Si^0(Idipp)][B(Ar^F)_4]$ (**1R**$[B(Ar^F)_4]$; R = H, Me, Et; Ar^F = C_6H_3-3,5-$(CF_3)_2$; Idipp = $C[N(C_6H_3$-2,6-$iPr_2)CH]_2)$ as red to orange colored, highly air-sensitive solids, which were characterized by single-crystal X-ray diffraction, IR spectroscopy and multinuclear NMR spectroscopy. Dynamic NMR studies in solution revealed a degenerate isomerization (topomerization) of the "σ-bonded" tautomers of **1H**$[B-(Ar^F)_4]$, which proceeds according to quantum chemical calculations via a NHC-stabilized (NHC = N-heterocyclic carbene) disilahydronium ion ("π-bonded" isomer) and is reminiscent of the degenerate rearrangement of carbenium

ions formed upon protonation of olefins. The topomerization of **1H**$[B(Ar^F)_4]$ provides the first example of a reversible 1,2-H migration along a Si=Si bond observed in a molecular system. In contrast, **1Me**$[B(Ar^F)_4]$ adopts a "rigid" structure in solution due to the higher energy required for the interconversion of the "σ-bonded" isomer into a putative NHC-stabilized disilamethonium ion. Addition of alkali metal borates to **1** afforded the alkali metal disilicon(0) borates **1M**$[BAr_4]$ (M = Li, Ar = C_6F_5; M = Na, Ar = Ar^F) as brown, air-sensitive solids. Single-crystal X-ray diffraction analyses and NMR spectroscopic studies of **1M**$[BAr_4]$ suggest in concert with quantum chemical calculations that encapsulation of the alkali metal cations in the cavity of **1** predominantly occurs via electrostatic cation−π interactions with the Si=Si π-bond and the peripheral NHC aryl rings. Displacement of the [Si(NHC)] fragments by the isolobal fragments [PR] and $[SiR]^−$ interrelates the cations $[(NHC)(R)Si=Si(NHC)]^+$ to a series of familiar, multiply bonded Si and P compounds as verified by analyses of their electronic structures.
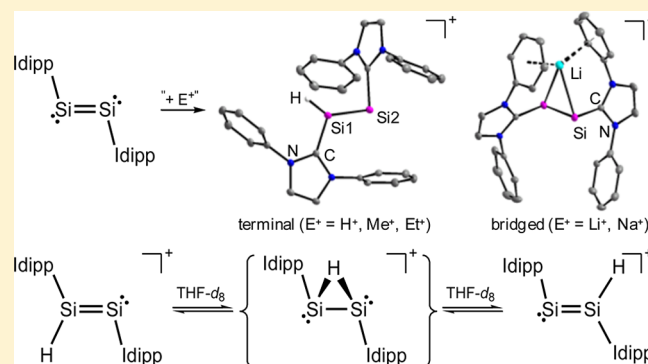
1. INTRODUCTION

Stabilization of highly reactive low-valent main-group element species by utilizing N-heterocyclic carbenes (NHCs) as particularly strong σ-donors led in recent years to a plethora of novel compounds with intriguing synthetic potential and to a flourishing, rapidly developing field in chemistry.[1] Appealing examples in low-valent silicon chemistry include the Si^0 compounds (Idipp)Si=Si(Idipp) (**1**, Idipp = $C[N(dipp)CH]_2$, dipp = C_6H_3-2,6-$iPr_2)^2$ and Si(bNHC) (bNHC = bidentate N-heterocyclic carbene),[3] the Si^I halides $Si_2X_2(Idipp)_2$ (X = Cl,[2] Br,[4] I[4]), the NHC-adducts of the Si^{II} halides SiX_2 (X = Cl−I),[5] $Si(X)R$ (X = Cl, H; R = aryl, amino),[6] and of the disilenylsilylene $SiR(SiR=SiR_2)$,[7] or the NHC-stabilized cations $[Si_2]^+$,[8] $[SiR]^+$ and Si^{2+}.[5d,6e,9] The same strategy also enabled the trapping of silagermenylidenes $(R_2Si=Ge)$,[10] phosphasilenylidenes $(RP=Si)^{11}$ and disilavinylidenes $(R_2Si=Si)$.[12]

Analysis of the bonding between main-group elements and NHCs raised a controversial debate in the literature.[13] G. Frenking et al. viewed **1** as a Si_2 molecule that is trapped in its excited $(^1\Delta_g)$ electronic state by two NHCs, and calculated the donor−acceptor $Si−C_{NHC}$ interactions in **1** using the

NOCV method.[14] Although this donor−acceptor model provides a simplified interpretation of the bonding in **1**, which has been also used to rationalize the bonding in other NHC-stabilized diatomic molecules,[14,15] it is not adequate to forecast the reactivity of **1** given the considerably higher energy of the $(^1\Delta_g)$ electronic state of Si_2 than that of its triplet ground-state configuration $(X^3\Sigma_g^-)^{16}$ and the rather large $Si−C_{NHC}$ bond dissociation energies,[17] which prevented so far the use of **1** as a source of Si_2 in reactions.

An alternative view of **1** was recently presented in an experimental and theoretical study by our group, which uncovered the similarity of the electronic structure of **1** with that of the diphosphene (E)-Mes*P=PMes* (Mes* = C_6H_2-2,4,6-tBu_3) and the NHC-stabilized phosphasilenylidene (Idipp)Si=PMes*, with all three compounds showing a similar sequence of the frontier orbitals with almost isoenergetic $n_+(E−E)$ lone pair (E = Si or P)[18] and $\pi(E=E)$ orbitals as the HOMO and the HOMO−1, respectively.[11] This relationship, which can be traced back to the isolobal analogy[19] of the

fragments [Si(NHC)], [PR] and [SiR]⁻, allowed also to rationalize the experimentally determined structure of the 1e-oxidation product of **1** ([Si₂(Idipp)₂]⁺), and to interrelate its electronic structure with that of the disilyne radical anions [Si₂R₂]⁻.[8,20]

Additional support for this view can be found by comparing the reactivity of the isolobal compounds. Remarkably, diphosphenes have been shown to adopt either η^1, η^2 or $\mu(\eta^1;\eta^1)$ coordination modes in complexes with coinage-metals,[21] and similar coinage metal complexes of the disilicon(0) compound **1** of the general formulas [MCl(η^1-**1**)], [M(η^2-**1**)][B(C₆F₅)₄] and [M₂Cl₂-μ-(1κSi¹:2κSi²-**1**)] (M = coinage metal atom) have been reported recently by G. Robinson et al. and our group.[22]

In comparison, reactivity studies of diphosphenes toward simple electrophiles such as H⁺ or R⁺ are very limited. Methylation of (E)-Mes*P═PMes* has been reported to give the isolable phosphanylphosphenium cation [Mes*(Me)P═PMes*]⁺,[23a] whereas attempts to detect the corresponding protonation product [Mes*(H)P═PMes*]⁺ failed.[21b,23b]

This prompted us to study the hitherto unexplored reactivity of **1** toward the electrophiles H⁺ and R⁺ and alkali metal cations. Herein, we report on the protonation and electrophilic alkylation of **1** leading to the disilicon(I) compounds [(Idipp)(R)Si═Si(Idipp)]A (R = H, Me, Et; A = borate anion) as well as the reactions of **1** with alkali metal borates, yielding the alkali metal disilicon(0) borates [Si₂(M)(Idipp)₂]A (M = Li, Na). All products were thoroughly studied by a combination of experimental and theoretical methods. In addition, we report on a detailed quantum chemical study, which corroborates the isolobal analogy of the cations [(Idipp)(R)Si═Si(Idipp)]⁺ to a series of familiar, multiply bonded Si and P compounds.

2. RESULTS AND DISCUSSION

2.1. Protonation of (Idipp)Si═Si(Idipp). The hydridodisilicon(I)-borate [(Idipp)(H)Si═Si(Idipp)][B-(Ar^F)₄] (**1H**[B(Ar^F)₄]) was obtained selectively upon protonation of **1** with Brookhart's acid ([H(Et₂O)₂][B(Ar^F)₄], Ar^F = C₆H₃-3,5-(CF₃)₂)[24] in fluorobenzene and isolated after crystallization from a fluorobenzene/*n*-hexane mixture at −30 °C as a dark red, highly air-sensitive solid in 80% yield (Scheme 1) (see Supporting Information (SI), chapter 2.1). Compound

Scheme 1. Synthesis of Compound 1H[B(Ar^F)₄][a]
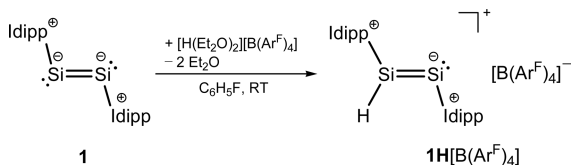
[a]Formal charges are encircled.

1H[B(Ar^F)₄] is a thermally robust solid, which decomposes upon melting in a vacuum-sealed glass capillary at 221 °C. Slow decomposition of **1H**[B(Ar^F)₄] to [IdippH][B(Ar^F)₄] and other unidentified products was however observed by ¹H NMR spectroscopy in THF-*d*₈ solution at room temperature within 24 h.

The solid-state structure of **1H**[B(Ar^F)₄] was determined by single-crystal X-ray diffraction, and confirmed that the cations **1H**⁺ (Figure 1) are well separated from the borate anions. The

closest Si···F contacts of 4.99(1) Å are significantly longer than the sum of the van der Waals radii of silicon and fluorine (3.6 Å).[25] The H85 atom was localized in the difference Fourier map and isotropically refined. It is σ-bonded to the Si1 atom, which is trigonal planar bonded according to the sum of bond angles of 360(1)°. The torsion angles C1−Si1−Si2−C28 and H85−Si1−Si2−C28 of 177.61(8)° and −6(1)° indicate a planar C_NHC−Si(H)−Si−C_NHC core with a *trans*-arrangement of the NHC substituents. The Si1-bonded central ring of the NHC substituent adopts a coplanar conformation (φ_{NHC1} = 8.60(6)°) with respect to the C_NHC−Si−Si−C_NHC plane, whereas the Si2-bonded NHC-substituent is perpendicularly oriented (φ_{NHC2} = 71.06(6)°) (Figure 1, right).[26]

The Si═Si bond (2.1873(8) Å) of **1H**⁺ compares well with those of the isolobal compounds (Z)-Tbb(Br)Si═Si(SIdipp) (2.167(2) Å, Tbb = C₆H₂-2,6-[CH(SiMe₃)₂]₂-4-*t*Bu, SIdipp = C[N(dipp)CH₂]₂),[12] (IMe₄)(R^Si)Si═SiR^Si (2.1989(6) Å, IMe₄ = C[N(Me)CMe]₂, R^Si = Si*i*Pr[CH(SiMe₃)₂]₂),[27] [Li(dme)₃]-[R^Si(H)Si═SiR^Si] (2.2034(9) Å, dme =1,2-dimethoxy-ethane)[28] and [(Idipp)(I)Si═Si(Idipp)][B(C₆F₅)₄] (2.1739(9) Å),[4] but is shorter (1.9%) than that of **1** (2.229(1) Å)[2] and Si₂(SIdipp)₂ (2.2323(8) Å).[29] Shortening of the Si═Si bond of **1** upon protonation can be rationalized according to comparative natural bonding orbital (NBO) analyses of **1**_calc and **1H**⁺_calc (see SI, Tables S7 and S8) with the increased s-character of the hybrid orbital on the Si1 atom employed in the Si−Si σ-bond. Consistently, **1H**⁺ displays a shortened Si1−C1 bond (1.882(2) Å) and a widened C1−Si1−Si2 angle (116.73(7)°) compared to **1** (Si−C_NHC: 1.927(2) Å; ∠C_NHC−Si−Si# = 93.37(5)°).[2] Another salient feature of the structure of **1H**⁺ is the narrow C28−Si2−Si1 angle of 95.34(6)°, which suggests the presence of a lone pair of high s-character at the Si2 atom, in full agreement with the results of the NBO analysis of **1H**⁺_calc (see SI, Table S8).

The ATR FTIR spectrum of a solid state sample of **1H**[B(Ar^F)₄] displays a weak absorption band at 2142 cm⁻¹, which is assigned to the ν(Si−H) stretching vibration (see SI, Figure S1). This band does not appear in the IR spectrum of the deuterated derivative [(Idipp)(D)Si═Si(Idipp)][B(Ar^F)₄] (**1D**[B(Ar^F)₄]), which was analogously obtained from **1** and [D(Et₂O)₂][B(Ar^F)₄] (see SI, chapter 2.2). However, the ν(Si−D) absorption band of **1D**[B(Ar^F)₄], which is expected to appear at 1541 cm⁻¹, was not detected due to its weak intensity and superimposition with other absorption bands in this region. The ν(Si−H) absorption band of **1H**[B(Ar^F)₄] emerges at a similar wavenumber as the ν(Si−H) absorptions of the 1,2-dihydridodisilenes (E)-Si₂H₂R₂ (ν(Si−H) = 2160 cm⁻¹, R = Bbp = C₆H₃-2,6-[CH(SiMe₃)₂]₂; ν(Si−H) = 2151 cm⁻¹, R = Bbt = C₆H₂-2,6-[CH(SiMe₃)₂]₂-4-C(SiMe₃)₃, both in KBr),[30] but appears at lower wavenumbers than those of hydridosilanes (e.g., RSiH_nCl_{3−n} (n = 1−3): ν(Si−H) = 2171−2240 cm⁻¹; R = C₆H₃-2,6-(C₆H₂-2,4,6-*i*Pr₃)₂).[31]

Notably, **1H**[B(Ar^F)₄] is fluxional on the NMR time scale. The dynamic process was studied by variable temperature ¹H, ¹³C{¹H} and ²⁹Si NMR spectroscopy in THF-*d*₈ and involves a degenerate isomerization (topomerization)[32] between the "σ-bonded" tautomers of **1H**⁺, which leads to an exchange of the two heterotopic silicon sites in solution (Scheme 2). Thus, two well separated ²⁹Si doublet signals at δ = 69.4 and 125.4 ppm are observed in the slow exchange limit ²⁹Si NMR spectrum of **1H**[B(Ar^F)₄] in THF-*d*₈ at 213 K for the three-coordinated (Si1) and two-coordinated (Si2) silicon atom, respectively (Figure 2, left). In comparison, no ²⁹Si NMR signal was
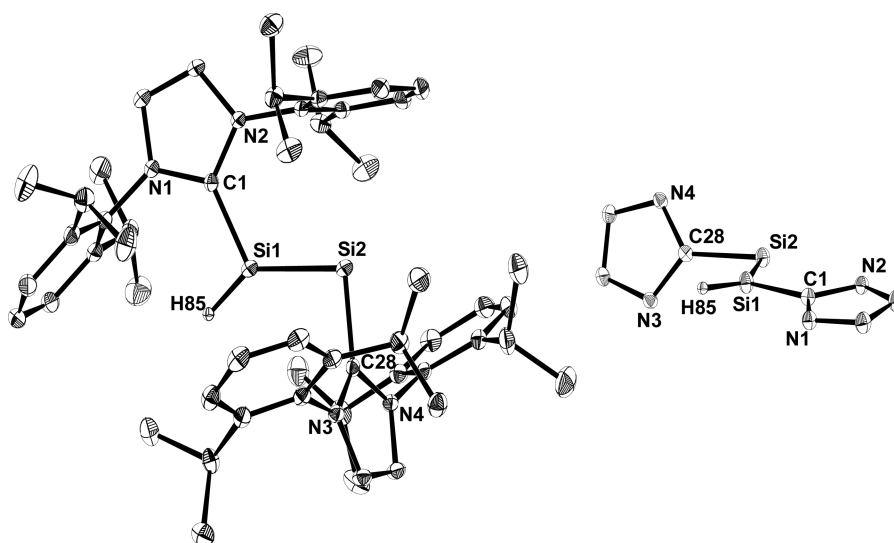
Figure 1. Left: DIAMOND plot of the molecular structure of the cation **1H$^+$** in the crystal lattice of **1H[B(Ar^F)$_4$]** at 123(2) K. Thermal ellipsoids are set at 30% probability. Hydrogen atoms, except the Si1-bonded H85 atom, were omitted for clarity. Selected bond lengths [Å], bond angles [deg] and torsion angles [deg]: Si1−C1 1.882(2), Si1−Si2 2.1873(8), Si2−C28 1.940(2), Si1−H85 1.32(2); C1−Si1−Si2 116.73(7), C1−Si1−H1 106(1), Si2−Si1−H85 138(1), C28−Si2−Si1 95.34(6); C1−Si1−Si2−C28 177.61(8), H85−Si1−Si2−C28 −6(1). Right: Different view of **1H$^+$** illustrating the different orientation of the Si-bonded NHC rings; hydrogen atoms (except the H85 atom) and the N-bonded dipp substituents were omitted for clarity.

Scheme 2. Topomerization of 1H[B(Ar^F)$_4$] in THF-d_8 Solution^a
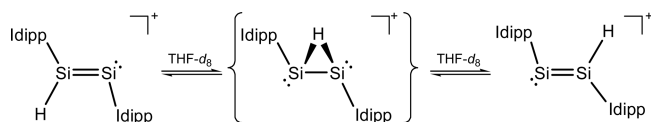
^{a}The tentative intermediate, a NHC-stabilized disilahydronium ion, is depicted in curly brackets. The [B(Ar^F)$_4$]$^−$ counteranion and formal charges were omitted for simplicity.

detected in the ^{29}Si NMR spectrum of **1H[B(Ar^F)$_4$]** in THF-d_8 at 333 K, even after long accumulation time, due to rapid site exchange.

Both ^{29}Si NMR signals of **1H[B(Ar^F)$_4$]** appear in the slow exchange limit spectrum at similar frequencies as those of the structurally related cations **1Me$^+$** and **1Et$^+$** (see Table 1 and chapter 2.2), but at a considerably higher field than that of **1** (δ = 224.5 ppm in C$_6$D$_6$).[2] The $^1J(^{29}$Si,^{1}H) (204.2 Hz) and $^2J(^{29}$Si,^{1}H) (14.8 Hz) coupling constants compare well with those of the 1,2-dihydridodisilenes (E)-Si$_2$H$_2$R$_2$ (R = Bbp, Bbt; $^1J(^{29}$Si,^{1}H) = 216 and 210 Hz, respectively; $^2J(^{29}$Si,^{1}H) = 16 Hz in both compounds),[30] indicating an increased s-character of the Si hybrid orbital involved in the Si−H bond in full agreement with the NBO analysis results of **1H$^+$** (see SI, Table S8).

Additional evidence for the dynamic process was provided by the slow exchange limit ^{1}H and ^{13}C{^{1}H} spectra of **1H[B-(Ar^F)$_4$]** (THF-d_8, 213 K), which display a double set of signals
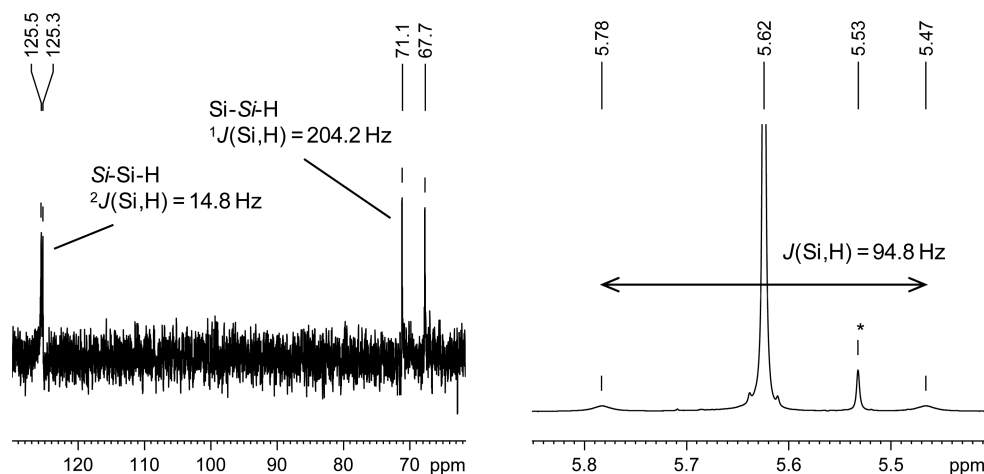
Figure 2. Left: ^{29}Si NMR spectrum of **1H[B(Ar^F)$_4$]** at 213 K displaying two doublets with characteristic $^1J(^{29}$Si,^{1}H) and $^2J(^{29}$Si,^{1}H) coupling constants. Right: Excerpt of the ^{1}H NMR spectrum of **1H[B(Ar^F)$_4$]** at 25 °C displaying the Si-H resonance at δ = 5.62 ppm with a mean $J(^{29}$Si,^{1}H) coupling constant due to the positional exchange of the Si sites; the signal marked with an asterisk originates from a small amount of an unknown impurity.

Table 1. Comparison of Selected NMR Data of the Cations 1R⁺ in 1R[BAr₄] (R = H, Me, Et, Na: Ar = Ar^F; R = I, Li: Ar = C₆F₅) and 1

	$\delta(^{29}\text{Si})$ [ppm]		$\delta(\text{C}_{\text{NHC}})$ [ppm]	
	Si1	Si2	C$_{\text{NHC}}$–Si1–R	C$_{\text{NHC}}$–Si2
1H⁺	69.4[c]	125.4[c]	161.8[c]	174.5[c]
1Me⁺	102.8[d]	115.2[d]	162.9[d]	177.1[d]
	103.0[e]	117.1[e]		
1Et⁺	111.6[d]	87.2[d]	164.2[d]	176.1[d]
1I⁺[a]	−26.4[f]	75.3[f]	153.6[f]	172.2[f]
1Li⁺	301.1[g]	301.1[g]	188.8[g]	188.8[g]
1Na⁺	288.8[g]	288.8[g]	189.1[g]	189.1[g]
1[b]	224.5[h]	224.5[h]	196.3[h]	196.3[h]

[a]Data taken from ref 4. [b]Data taken from ref 2. [c]THF-d_8, 213 K. [d]THF-d_8, 298 K. [e]C₆H₅F, 298 K. [f]THF-d_8, 203 K. [g]C₆D₅Cl, 298 K. [h]C₆D₆, 298 K.

for the heterotopic Idipp substituents, whereas the fast exchange limit ¹H and ¹³C{¹H} spectra of 1H[B(Ar^F)₄] (THF-d_8, 333 K) reveal only one set of signals (see SI, Figures S2−S7). The number and relative intensities of the Idipp signals in the slow exchange ¹H and ¹³C{¹H} NMR spectra clearly indicate that both NHC groups rotate fast about the Si−C$_{\text{NHC}}$ bonds on the NMR time scale. Most distinctive are the signals of the C$_{\text{NHC}}$ nuclei in the ¹³C{¹H} NMR spectra (Table 1). The signal of the Si1-bonded C$_{\text{NHC}}$ atom appears at lower frequency (δ = 161.8 ppm) than that of the Si2-bonded C$_{\text{NHC}}$ atom (δ = 174.5 ppm), and both C$_{\text{NHC}}$ atoms have a chemical shift in between that of Idipp (δ = 220.6 ppm in C₆D₆)[33] or 1 (δ = 196.3 in C₆D₆)[2] and the imidazolium salt (IdippH)Cl (δ = 139.3 ppm in DMSO-d_6).[5b] The same trend is observed for 1Me[B(Ar^F)₄] and 1Et[B(Ar^F)₄] and suggests a higher "imidazolium character" of the Si1-bonded NHC ring than that of the Si2-bonded NHC in 1R[B(Ar^F)₄] (R = H, Me, Et) (Table 1).

Topomerization of 1H[B(Ar^F)₄] involves an intramolecular 1,2-H migration and proceeds according to quantum chemical calculations (chapter 2.3) via an NHC-stabilized disilahydronium intermediate (Scheme 2). Evidence for the intramolecularity of the process was provided by the ²⁹Si satellite signals of the Si-H resonance in the ¹H NMR spectrum of 1H[B(Ar^F)₄] in THF-d_8 at 298 K (δ = 5.62 ppm), which displays an averaged $J(^{29}\text{Si},^1\text{H})$ coupling constant of 94.8 Hz (Figure 2, right).[34] A similar topomerization process has been proposed by G. Robinson et al. for the copper complex [CuCl(η^1-1)], however without unambiguous experimental verification.[22a] Furthermore, recent studies in our group have shown that the cation [(Idipp)(I)Si=Si(Idipp)]⁺ and the coinage metal complexes [MCl(η^1-1)] and [M(η^1-1)(PMe₃)]-[B(Ar^F)₄] (M = Cu, Ag, Au) undergo the same intramolecular topomerization process in solution as observed for 1H[B-(Ar^F)₄].[4,22b−d]

The thermodynamic parameters of the topomerization were obtained by full line-shape analysis of the NHC backbone C^{4,5}-H ring proton signals in the temperature range of 213−273 K and were found to be $\Delta H^{\neq}$ = 38.5($\pm$2.4) kJ mol⁻¹ and $\Delta S^{\neq}$ = −54.3($\pm$7.7) J K⁻¹ mol⁻¹ (see SI, chapter 3). Remarkably, the Gibbs energy of activation $\Delta G^{\neq}$ (51.6($\pm$0.6) kJ mol⁻¹ at T_c = 241 K, T_c = coalescence temperature) compares well with that calculated for the isomerization of the *trans*-bent disilene Si₂H₄ into the monohydrogen-bridged minimum structure (59 kJ mol⁻¹),[35] and the entropy of activation of the topomerization

of 1H[B(Ar^F)₄] is similar to that found for the intramolecular 1,2-hydrogen migration of the 1,2-dihydridodisilene (E)-Si₂H₂Bbt₂ (−63(8) J K⁻¹ mol⁻¹), which leads via a silylsilylene intermediate to a silane.[30]

The topomerization of 1H[B(Ar^F)₄] is the first example of a reversible 1,2-hydrogen migration observed along a Si=Si bond in a molecular system and provides a molecular model for the migration of hydrogen atoms on Si(001) surfaces via "dangling bonds" (i.e., coordinatively unsaturated silicon centers),[36] which is suggested to account for the decrease in efficiency of photovoltaic cells based on hydrogenated amorphous silicon (Staebler−Wronski effect).[37] Topomerization of 1H[B(Ar^F)₄] is reminiscent of that of diazenium ions in acidic solutions, which has been suggested to proceed either via an intra- or intermolecular H⁺ transfer,[38] and of the degenerate rearrangement of carbenium ions formed upon protonation of olefins.[39]

2.2. Alkylation of (Idipp)Si=Si(Idipp). Electrophilic alkylation of 1 was achieved upon treatment of 1 with the corresponding iodoalkane in the presence of Na[B(Ar^F)₄] to afford the mixed-valent alkyldisilicon(I) borates [(Idipp)(R)-Si^{II}=Si^0(Idipp)][B(Ar^F)₄] (1R[B(Ar^F)₄], R = Me, Et) (Scheme 3). Remarkably, addition of Na[B(Ar^F)₄] to a solution

Scheme 3. Electrophilic Alkylation of 1 to Give the Compounds 1R[B(Ar^F)₄] (R = Me, Et)[a]
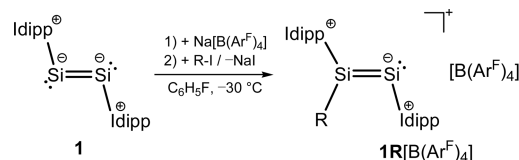
[a]Formal charges are encircled.

of 1 in fluorobenzene led to a color change from dark red to brown to afford selectively the alkalimetal disilicon(0) borate [Si₂(Na)(Idipp)₂][B(Ar^F)₄] (1Na[B(Ar^F)₄]) as discussed in chapter 2.4 (vide infra). Subsequent addition of the iodoalkane to the solution of 1Na[B(Ar^F)₄] in fluorobenzene was accompanied by a color change from brown to bright orange and precipitation of NaI leading selectively to the alkyldisilicon-(I) borate salts 1R[B(Ar^F)₄] (Scheme 3). Remarkably, preactivation of 1 via complexation of Na[B(Ar^F)₄] is not indispensable for the formation of the alkyldisilicon(I) cations 1R⁺, as evidenced by the reaction of 1 with iodomethane in C₆H₅F, which affords the analogous iodide salt [(Idipp) (Me)Si=Si(Idipp)]I according to ²⁹Si NMR spectroscopy. The salts 1R[B(Ar^F)₄] were isolated after crystallization from fluorobenzene/n-hexane mixtures at −30 °C as highly air-sensitive, orange solids in moderate yields (R = Me: 36%, R = Et: 50%) (see SI, chapters 2.3 and 2.4). Notably, 1 did not react with 2-iodopropane indicating that bulky electrophiles cannot access the sterically protected Si₂ core of 1. The compounds 1R[B(Ar^F)₄] are thermally robust and decompose upon melting in vacuum-sealed glass capillaries at elevated temperatures (R = Me: 213 °C, R = Et: 209 °C). As in the case of 1H[B(Ar^F)₄], the salts 1R[B(Ar^F)₄] decompose slowly in THF-d_8 solution at ambient temperature, the decomposition leading to [IdippH][B(Ar^F)₄] and other unidentified products.

Single-crystal X-ray diffraction analyses of 1Me[B(Ar^F)₄] and 1Et[B(Ar^F)₄] revealed that these compounds are isotypic with 1H[B(Ar^F)₄]. The cations 1R⁺ are well separated from the

borate anions as evidenced by the shortest Si···F distances of 5.416(5) Å ($1Me^+$) and 5.030(9) Å ($1Et^+$) (cf. $\Sigma r(Si\cdots F)_{vdW}$ = 3.6 Å),[25] and reveal similar structural features as $1H^+$, i.e., a *trans*-bent planar C_{NHC}−Si−Si−C_{NHC} core, in which a trigonal-planar coordinated Si1 atom (sum of angles at Si1: 359.6(1)° ($1Me^+$), 359.9(2)° ($1Et^+$)) is connected via a Si=Si bond to a V-shaped coordinated Si2 atom with a narrow angle at the Si2 atom (C28−Si2−Si1: 95.13(6)° ($1Me^+$), 100.08(7)° ($1Et^+$)) (Figure 3, Figure S34 (SI), Table 2). The Si·R (Si1−C56)
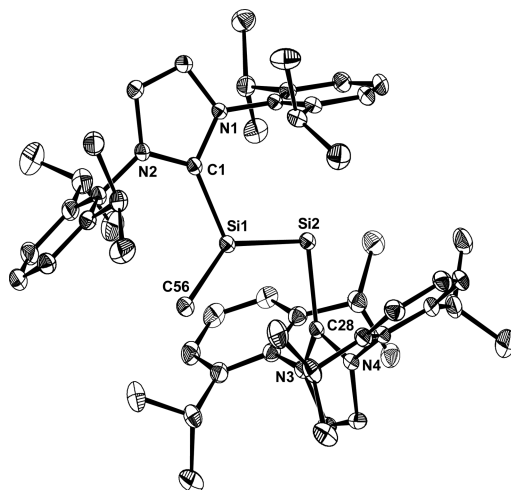
Figure 3. DIAMOND plot of the molecular structure of the cation $1Me^+$ in the crystal lattice of $1Me[B(Ar^F)_4]$ at 123(2) K. Thermal ellipsoids are set at 30% probability. Hydrogen atoms were omitted for clarity. Selected bond lengths [Å], bond angles [deg] and torsion angles [deg]: Si1−C1 1.901(2), Si1−Si2 2.1909(8), Si2−C28 1.947(2), Si1−C56 1.885(2); C1−Si1−Si2 114.62(7), C1−Si1−C56 111.3(1), Si2−Si1−C56 133.71(8), C28−Si2−Si1 95.13(6); C1−Si1−Si2−C28 −177.4(1), C28−Si2−Si1−C56 10.7(1).

bond lengths ($1Me^+$: 1.885(2) Å, $1Et^+$: 1.893(2) Å) are typical of Si−C single bonds and only slightly shorter than the Si1−C_{NHC} bond lengths ($1Me^+$: 1.901(2) Å, $1Et^+$: 1.912(2) Å). Whereas the Si2-bonded central ring of the NHC group adopts in all cases an almost orthogonal orientation with respect to the planar C_{NHC}−Si−Si−C_{NHC} core of the cations (φ_{NHC2} = 71.06(6)° ($1H^+$), 79.11(7)° ($1Me^+$), 88.03(7)° ($1Et^+$)),[26] the increasing bulkiness of the Si1-bonded substituent R in the series $1H^+$ → $1Me^+$ → $1Et^+$ provokes a conformational change of the Si1-bonded NHC substituent from an almost coplanar orientation in $1H^+$ (φ_{NHC1} = 8.60(6)°) and $1Me^+$ (φ_{NHC1} = 13.23(8)°) to a synclinal conformation in $1Et^+$ (φ_{NHC1} =

52.52(8)°). The increased steric bulk of the R group can also be invoked to rationalize the gradual elongation of the Si1−C1 bonds in the series $1H^+$ (1.882(2) Å) → $1Me^+$ (1.901(2) Å) → $1Et^+$ (1.912(2) Å) and the decrease of the C1−Si1−Si2 angles in the same series ($1H^+$ (116.73(7)°) → $1Me^+$ (114.62(7)°) → $1Et^+$ (108.36(7)°)) (Table 2).

In contrast to $1H[B(Ar^F)_4]$, multinuclear NMR spectroscopic studies of $1R[B(Ar^F)_4]$ (R = Me, Et) in THF-d_8 indicate that no degenerate isomerization (topomerization) of the "σ-bonded" isomers occurs in solution up to 333 K.[40] Thus, the ^1H and $^{13}C\{^1H\}$ NMR spectra display a double set of signals for the heterotopic Idipp substituents (see SI, Figures S12−S15 and S17−S21), which could be unequivocally assigned by a combination of ^1H−^{13}C HMQC, ^1H−^{13}C HMBC and ^1H−^{29}Si HMBC correlation spectroscopies using the correlation between the $C^{4,5}$-H proton signals of the NHCs and the ^{29}Si NMR signals. The number and relative intensity of the signals of each Idipp group indicates that both NHCs rotate fast about the respective Si−C_{NHC} bonds on the NMR time scale. Similarly, the ^{29}Si NMR spectra of $1R[B(Ar^F)_4]$ (R = Me, Et) in THF-d_8 show two separate resonances at 298 K (Table 1), which were unequivocally assigned by two-dimensional ^1H−^{29}Si HMBC spectroscopy. The ^{29}Si NMR spectrum of $1Me[B(Ar^F)_4]$ was also recorded in C_6H_5F and displayed two signals at 103.0 and 117.1 ppm (calibrated against SiMe$_4$), i.e., at almost the same position as those observed in THF-d_8 (102.8 and 115.2 ppm, respectively) (Table 1). This observation excludes a coordination of THF to the potentially electrophilic Si2-center of the cations $[(Idipp)(Me)Si=Si(Idipp)]^+$ in solution. Moreover, the ^{29}Si NMR chemical shifts of the corresponding iodide salt $1Me[I]$ in C_6H_5F (103.5 and 112.6 ppm) are quite similar to those of $1Me[B(Ar^F)_4]$ suggesting a negligible interaction of the stronger nucleophile I$^-$ with $1Me^+$.

A comparison of the ^{29}Si NMR chemical shifts of $1R^+$ reveals, that the three-coordinated Si nuclei (Si-R) are progressively deshielded in the series $1H[B(Ar^F)_4]$ (δ = 69.4 ppm) → $1Me[B(Ar^F)_4]$ (δ = 102.8 ppm) → $1Et[B(Ar^F)_4]$ (δ = 111.6 ppm) (Table 1). Notably, a similar, however less pronounced trend is observed in the series of the alkyl silanes SiMe$_3$R upon replacement of the R substituent (H (δ = −18.5 ppm) → Me (δ = 0.0 ppm) → Et (δ = 1.6 ppm)).[41] In comparison, the two-coordinated ^{29}Si NMR nuclei are progressively shielded in the same series $1H[B(Ar^F)_4]$ (δ = 125.4 ppm) → $1Me[B(Ar^F)_4]$ (δ = 115.2 ppm) → $1Et[B(Ar^F)_4]$ (δ = 87.2 ppm) (Table 1). Remarkably, a similar influence of the substituents R was observed on the ^{13}C NMR chemical shifts of the C^α and C^β atoms in the alkenes R-C^βH=C^αH$_2$ (R = H, Me, Et).[42]

Table 2. Comparison of Selected Bond Lengths [Å], Bond Angles [deg] and Dihedral Angles [deg] of the Cations $1R^+$ in $1R[BAr_4]$ (R = H, Me, Et, Na: Ar = Ar^F; R = I, Li: Ar = C_6F_5) and 1

	Si−Si [Å]	Si1−C_{NHC} [Å]	Si2−C_{NHC} [Å]	C_{NHC}−Si1−Si2 [deg]	C_{NHC}−Si2−Si1 [deg]	$\varphi_{NHC1}{}^a$ [deg]	$\varphi_{NHC2}{}^a$ [deg]
$1H^+$	2.1873(8)	1.882(2)	1.940(2)	116.73(7)	95.34(6)	8.60(6)	71.06(6)
$1Me^+$	2.1909(8)	1.901(2)	1.947(2)	114.62(7)	95.13(6)	13.23(8)	79.11(7)
$1Et^+$	2.1726(9)	1.912(2)	1.941(2)	108.36(7)	100.08(7)	52.52(8)	88.03(7)
$1I^{+b}$	2.1739(9)	1.901(2)	1.931(2)	112.83(7)	96.61(7)	96.69(7)	95.78(7)
$1Li^+$	2.234(1)	1.941(3)	1.938(3)	94.9(1)	98.7(1)	79.0(1)	108.9(1)
$1Na^+$	2.248(2)	1.948(4)	1.948(4)	95.4(1)	95.4(1)	87.7(1)	87.7(1)
1^c	2.229(1)	1.927(2)	1.927(2)	93.37(5)	93.37(5)	87.11(5)	87.11(5)

$^a\varphi_{NHC1}$ and φ_{NHC2} are the dihedral angles between the least-squares plane of the C_{NHC}−Si−Si−C_{NHC} atoms and the Si1- and Si2-bonded NHCs rings, respectively. ^{b}Data taken from ref 4. ^{c}Data taken from ref 2.
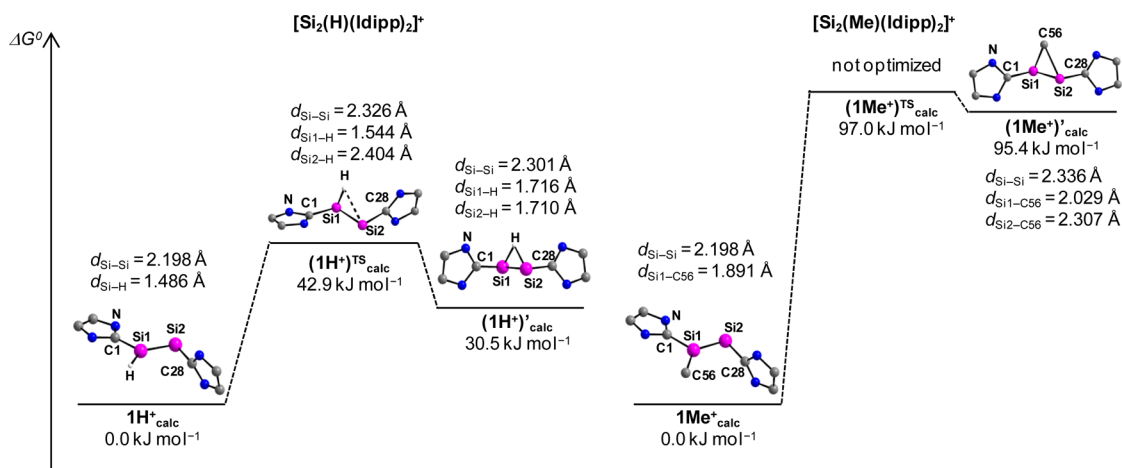
Figure 4. Schematic Gibbs profiles (T = 298 K) for the degenerate isomerizations of $[Si_2(H)(Idipp)_2]^+$ (left) and $[Si_2(Me)(Idipp)_2]^+$ (right), which includes the optimized minimum structures $1H^+_{calc}$, $1Me^+_{calc}$, $(1H^+)'_{calc}$ and $(1Me^+)'_{calc}$ and the transition state $(1H^+)^{TS}_{calc}$ with selected bonding parameters. The N-bonded dipp substituents and H atoms, except the Si-bonded H atom, were omitted for clarity, and only one-half of the symmetric energy profiles is depicted.

2.3. Quantum Chemical Studies of $1H^+$ and $1Me^+$. In order to get a closer insight into the topomerization of $1H^+$, the energy hypersurface of $1H^+$ was analyzed and compared with that of $1Me^+$ by quantum chemical calculations at the B97-D3 level of theory,[43a−d] including the COSMO solvation model[43e] and RI-JCOSX approximations (see SI, chapter 5).[43f,g] The def2-TZVP basis sets were used for the Si, N, heterocyclic C atoms and the Si1-attached H atom and methyl group, and the def2-SVP basis sets for all peripheral carbon and all other hydrogen atoms.[43h,i] The level of theory is abbreviated in the following as B97-D3/I.

Geometry optimization of $1H^+$ and $1Me^+$ afforded minimum structures with a Si1−H and Si1−Me σ-bond ("σ-bonded" isomers),[44] which are designated in the following as $1H^+_{calc}$ and $1Me^+_{calc}$. A comparison of the structural parameters revealed an excellent agreement between the calculated and the experimental bond lengths and angles obtained for $1H[B(Ar^F)_4]$ and $1Me[B(Ar^F)_4]$ by X-ray crystallography. Remarkably, also the quite different conformation of the Si1-bonded NHC compared to the Si2-bonded NHC could be well reproduced by the quantum chemical calculations (see SI, Tables S4 and S5).

A second minimum structure could be localized on the energy hypersurface of $1H^+$ and $1Me^+$, which is however less stable than that of $1H^+_{calc}$ and $1Me^+_{calc}$ by 30.5 kJ mol^{-1} and 95.4 kJ mol^{-1} (ΔG values at 298 K), respectively. $(1H^+)'_{calc}$ features a "symmetric" H-bridged structure, in which the H atom is located over the Si−Si bond at almost the same distance from the two Si atoms ("π-bonded" isomer).[44] Notably, the Si−Si bond of $(1H^+)'_{calc}$ (2.301 Å) is longer than the Si=Si bond of $1H^+_{calc}$ (2.198 Å), and its length approaches the Si−Si single bond length in α-Si (2.352 Å).[45] $(1H^+)'_{calc}$ features a 3c-2e Si−H−Si interaction, which leads to longer Si−H bonds (1.716 and 1.710 Å) than the 2c-2e Si−H bond (1.486 Å) of $1H^+_{calc}$ ("σ-bonded" isomer). The two minimum structures are connected via a transition state $(1H^+)^{TS}_{calc}$, which lies 42.9 kJ mol^{-1} higher in energy than $1H^+_{calc}$ (Figure 4). The calculated barrier agrees acceptably well with the experimentally derived Gibbs energy of activation ($\Delta G^{\neq}$(298 K) = 54.7 ± 0.2 kJ mol^{-1}). The conversion of $1H^+_{calc}$ to $(1H^+)'_{calc}$ involves a H-migration from the end-on to a bridging position and a concomitant rotation of the Si1-bonded heterocyclic ring from an almost coplanar orientation

in $1H^+_{calc}$ (φ_{NHC1} = 3.63°) to an almost orthogonal orientation in $(1H^+)'_{calc}$ (φ_{NHC1} = 76.17°) (see SI, Table S4).[26]

In contrast to $(1H^+)'_{calc}$, the second minimum structure ($(1Me^+)'_{calc}$) located on the energy hypersurface of $1Me^+$ reveals an asymmetric bridging of the Si−Si single bond (2.336 Å) by the methyl group, as evidenced by the markedly different Si1−C56 (2.029 Å) and Si2−C56 (2.307 Å) bonds (Figure 4). Both Si−C_{Me} bonds are longer than the 2c-2e Si−C_{Me} bond of the "σ-bonded" isomer $1Me^+_{calc}$ (1.891 Å). A relaxed potential energy surface scan was performed starting from $1Me^+_{calc}$, which involved a progressive decrease of the Si2−C_{Me} distance from 377 pm (the Si2−C_{Me} distance in $1Me^+_{calc}$) to 137 pm in 12 steps. This scan afforded a maximum, which displayed one imaginary frequency of −177 cm^{-1} and a Gibbs energy of 97 kJ mol^{-1}. Further optimization of this structure did not furnish the transition state $(1Me^+)^{TS}_{calc}$, but instead led to the minimum structures $1Me^+_{calc}$ and $(1Me^+)'_{calc}$ indicating a flat progression of the potential energy surface during interconversion of $(1Me^+)'_{calc}$ into the overall minimum structure $1Me^+_{calc}$ (Figure 4). The significantly higher energy barrier for the transformation of $1Me^+_{calc}$ into $(1Me^+)'_{calc}$ compared to that of $1H^+$ confirms the observed rigidity of $1Me^+$ on the NMR time scale.

NBO (natural bond orbital) analyses of the "σ-bonded" isomers $1H^+_{calc}$ and $1Me^+_{calc}$ revealed a localized Si1−R (R = H, Me) σ-bond NBO, a Si−Si σ- and π-bond NBO, which are both polarized toward the Si1 atom, and a lone pair of electrons at Si2 in a natural hybrid orbital (NHO) with high s-character (ca. 77%) (see SI, Tables S8 and S10).[43j] The rather high Wiberg bond Index (WBI) of the Si=Si bond of 1.61 ($1H^+_{calc}$) and 1.62 ($1Me^+_{calc}$) and the high covalent contribution to the overall NRT (natural resonance theory) Si−Si bond order of 1.85 ($1H^+_{calc}$) and 1.84 ($1Me^+_{calc}$) provide additional support for the presence of a slightly polar, covalent Si=Si bond.

Natural population analyses of $1H^+_{calc}$ and $1Me^+_{calc}$ revealed a considerable electron transfer from **1** to the electrophile (H$^+$, Me$^+$), leading to a negative partial charge at the H atom (q = −0.14e) and the methyl group (q = −0.38e). The charge flow occurs mainly from the Si atoms, as evidenced by a comparison of the Si partial charges in $1H^+_{calc}$ (q(Si1) = 0.31e, q(Si2) = 0.26e) and $1Me^+_{calc}$ (q(Si1) = 0.65e, q(Si2) = 0.20e) with those in 1_{calc} (q(Si1,Si2) = −0.10e) (see SI, Tables S7, S8 and S10).

$d_{Si1-H} = 1.716$ Å
$d_{Si2-H} = 1.710$ Å
$d_{Si1-Si2} = 2.301$ Å
$\angle_{Si1-H-Si2} = 84.39°$

3c-2e Si-H-Si bond

$d_{C56-H1} = 1.125$ Å
$d_{C56-H2} = 1.088$ Å
$d_{C56-H3} = 1.083$ Å
$d_{Si2-H1} = 2.030$ Å
$d_{Si1-Si2} = 2.336$ Å
$\angle_{Si1-C56-S2} = 51.81°$
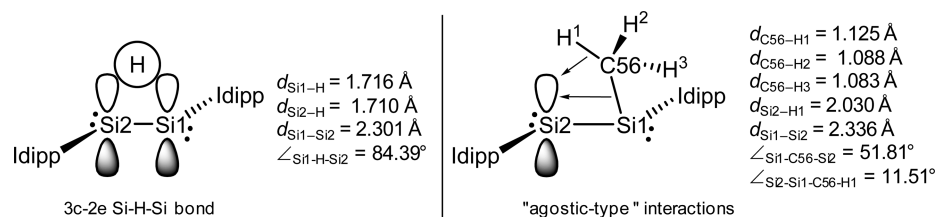$\angle_{S2-Si1-C56-H1} = 11.51°$

"agostic-type" interactions

Figure 5. Schematic presentation of the Si−R−Si interaction in the "π-coordinated" isomers of (1H⁺) (left) and 1Me⁺ (right) according to NBO analyses with selected bonding parameters.

In comparison, the "π-bonded" isomers $(1H^+)'_{calc}$ and $(1Me^+)'_{calc}$ display only one nonpolarized NBO corresponding to the Si−Si σ-bond, with each Si atom carrying a lone pair of electrons in a NHO with high s-character (see SI, Tables S9 and S11). This leads to a considerably lower Si−Si WBI $((1H^+)'_{calc}: 1.01; (1Me^+)'_{calc}: 0.90)$ than those of $1H^+_{calc}$ and $1Me^+_{calc}$ and to a Si−Si NRT bond order $((1H^+)'_{calc}: 0.96; (1Me^+)'_{calc}: 0.90)$, which lies at half the value of that in the "σ-bonded" isomers $1H^+_{calc}$ and $1Me^+_{calc}$. All these results suggest the presence of a Si−Si single bond in $(1H^+)'_{calc}$ and $(1Me^+)'_{calc}$.

The largest difference between $(1H^+)'_{calc}$ and $(1Me^+)'_{calc}$ exists with respect to the Si-R-Si interaction. In $(1H^+)'_{calc}$, a highly localized NBO is found corresponding to the 3c-2e Si−H−Si interaction, which is formed of an almost pure 3p NHO of each Si atom and the hydrogen 1s orbital and is polarized toward the H atom (Figure 5, left). In comparison, only a NBO for the $\sigma(Si1−C_{Me})$ bond, but no NBO for the $Si2−C_{Me}$ bond was found in $(1Me^+)'_{calc}$ (see SI, Table S11). Instead, the Si2 atom bears a lone vacancy of pure p-character (with an occupancy of 0.26 electrons), which attains electron density from the $\sigma(Si1−C_{Me})$ and one $\sigma(C−H)$ orbital of the methyl group according to second order perturbation theory. The corresponding second order perturbation energies $E^{(2)}$ amount to 196.6 kJ mol⁻¹ and 156.9 kJ mol⁻¹, respectively. This "agostic-type" interaction locates one of the methyl hydrogen atoms (H1) in the Si2−Si1−C56 plane and leads to an elongation of one C_{Me}−H1 (C56−H1) bond reducing the electron deficiency at the Si2 atom (Figure 5, right).

2.4. Addition of Alkali Metal Borates to (Idipp)Si═Si(Idipp). During the syntheses of $1R[B(Ar^F)_4]$ (R = Me, Et) from 1, $Na[B(Ar^F)]_4$ and RI, a color change of the dark red solution of 1 in C_6H_5F to brown was observed upon treatment with $Na[B(Ar^F)_4]$. This stimulated us to study the interaction of 1 with alkali metal cations. In fact, compound 1 readily reacted with the alkali metal borates $[Li(Et_2O)_{2.5}][B(C_6F_5)_4]$[46] and $Na[B(Ar^F)_4]$[24b,47] to afford after crystallization from fluorobenzene/n-hexane mixtures the alkali metal disilicon(0) borates $[Si_2(M)(Idipp)_2][BAr_4]$ ($1M[BAr_4]$; M = Li, Ar = C_6F_5; M = Na, Ar = Ar^F) as brown solids in 43% (M = Li) and 70% yield (M = Na), respectively (Scheme 4) (see SI, chapters 2.5 and 2.6). The compounds rapidly decompose upon contact with air, but are thermally quite robust solids (decomposition at 202 °C ($1Li[B(C_6F_5)_4]$) and 211−212 °C ($1Na[B(Ar^F)_4]$)).

Dissolution of $1M[BAr_4]$ (M = Li, Na) in coordinating solvents, such as diethyl ether or THF, led to an instant decomplexation of the alkali metal ions to give back 1 and the alkali metal borates. However, solutions of $1M[BAr_4]$ in noncoordinating polar solvents (fluorobenzene, chlorobenzene) were found to be stable for several days at room temperature.

Scheme 4. Synthesis of the Alkali Metal Disilicon(0) Borates $1M[BAr_4]$ (M = Li, Ar = C_6F_5, n = 2.5; M = Na, Ar = Ar^F, n = 0)[a]
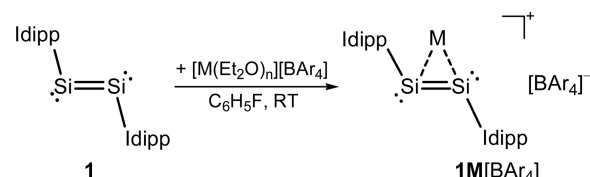
[a]Formal charges and the η^6-coordination of the two N-bonded dipp substituents are not depicted.

The solid state structures of $1Li[B(C_6F_5)_4]\cdot(n-C_6H_{14})$ (Figure 6) and $1Na[B(Ar^F)_4]$ (see SI, Figure S35) were
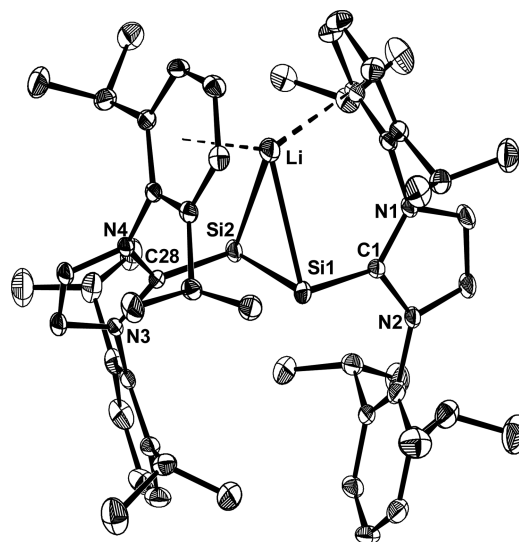
Figure 6. DIAMOND plot of the molecular structure of 1Li⁺ in the crystal lattice of $1Li[B(C_6F_5)_4]\cdot(n-C_6H_{14})$ at 123(2) K. Thermal ellipsoids are set at 30% probability. Hydrogen atoms were omitted for clarity. Selected bond lengths [Å], bond angles [deg] and torsion angles [deg]: C1−Si1 1.941(3), C28−Si2 1.938(3), Li−Si1 2.822(6), Li−Si2 2.925(7), Si1−Si2 2.234(1); Si1−Li−Si2 45.7(1), C1−Si1−Si2 94.9(1), C1−Si1−Li 95.9(2), Si2−Si1−Li 69.6(1), C28−Si2−Si1 98.7(1), C28−Si2−Li 93.7(2), Si1−Si2−Li 64.7(1); C1−Si1−Si2−C28 175.5(1).

determined by single-crystal X-ray diffraction studies. The C_1-symmetric cations 1Li⁺ and C_2-symmetric cations 1Na⁺ are well separated from the borate counteranions, as apparent from the shortest Si⋯F distances of 6.155(3) Å and 6.809(6) Å, respectively (cf. $\Sigma r(Si\cdots F)_{vdW} = 3.6$ Å).[25] The alkali metal cations are encapsulated in the cavity of the (Idipp)Si═Si(Idipp) core of 1Li⁺ and 1Na⁺ via η^2-coordination to the Si═Si π-bond and η^6-coordination to two peripheral 2,6-

Scheme 5. Isolobal Derivatives of the Cations $[(NHC)(R)Si^{II}{=}Si^{0}(NHC)]^{+}$ (A; A = $1R^{+}$ for NHC = Idipp and R = H, Me, Et)
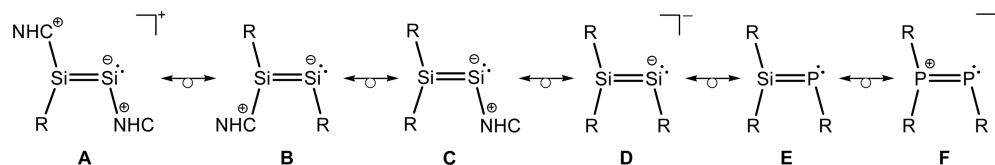
diisopropylphenyl (dipp) rings (Figure 6 and Figure S35 (SI)). The Si−Li bond distances in $1Li^{+}$ (Si1−Li: 2.822(6) Å, Si2−Li: 2.925(7) Å) are quite long and comparable to that of the contact ion pair $R_2Si{=}Si(R)Li(dme)_2$ (2.853(3) Å, R = C_6H_2-2,4,6-iPr$_3$).[48] They suggest a weak Si···Li interaction, which is corroborated by the only slightly elongated Si=Si bond (2.234(1) Å, 0.2%) compared to **1** (2.229(1) Å).[2] The Si−Na bond lengths in $1Na^{+}$ (3.096(3) Å) are similar to the Si−Na bond lengths in the dimer $(NaSitBu_3)_2$ (3.060(4) and 3.073(4) Å),[49] and the Si=Si bond (2.248(2) Å) of $1Na^{+}$ is slightly more elongated (0.9%) than in $1Li^{+}$.

Encapsulation of the Li^{+} and Na^{+} ions in the cavity of **1** leads only to minor structural changes of the (Idipp)Si=Si(Idipp) core (Table 2). This suggests a mainly electrostatic bonding of the alkali metal ions to the Si=Si π bond and the π-electron systems of the two dipp substituents, which is typical for alkali metal cation−π interactions.[50] Notably the M−arene$_{centroid}$ distances (2.292 and 2.451 Å in $1Li^{+}$, 2.557 Å in $1Na^{+}$), compare well with those of the alkali metal cation−π complexes $[Li(\eta^6$-toluene)][CB$_{11}$Me$_{12}$] (2.39, 2.45 Å) and $[Na(\eta^6$-benzene)$_2$][CB$_{11}$Me$_{12}$] (2.69 and 2.71 Å).[51] Remarkably, a similar reaction of the diboron(0) compound (Idipp)B≡B(Idipp) with alkali metal borates was reported recently to give the cations $[B_2(M)(Idipp)_2]^{+}$ (M = Li, Na), which however could not be isolated and structurally characterized.[52]

Multinuclear NMR spectroscopic analyses of $1M[BAr_4]$ in C_6D_5Cl indicate clearly that the encapsulation of the alkali metal cations is retained in solution. Thus, the $^{29}Si\{^1H\}$ NMR spectrum of $1Li[B(C_6F_5)_4]$ displays one broadened signal at 301.1 ppm and that of $1Na[B(Ar^F)_4]$ one sharp ^{29}Si NMR signal at 288.8 ppm (see SI, Figures S26 and S30). Both ^{29}Si NMR resonances appear at considerably lower field compared to **1** (δ = 224.5 ppm).[2] Remarkably, the opposite trend was observed for the ^{29}Si NMR resonances of η^2-disilene complexes of transition metals, which can be explained by the considerable metal−ligand π back-bonding in the latter compounds.[53] No coupling between the ^{29}Si (I = 1/2) and the quadrupolar ^7Li (I = 3/2) nucleus could be resolved in the $^{29}Si\{^1H\}$ NMR spectrum of $1Li[B(C_6F_5)_4]$ at 298 and 243 K, due to signal broadening. However, the width of the ^{29}Si NMR signal of $\Delta\nu \approx$ 56 Hz (298 K) suggests, that the upper limit of the scalar ^{29}Si−^7Li coupling would be 14 Hz. This value is considerably smaller than those in lithiosilanes ($^1J(^{29}Si,^7Li)$ = 32.8−65.3 Hz),[54] providing additional evidence for the mainly electrostatic interaction of the alkali metal ions with the Si=Si π-bond in $1M[BAr_4]$. Notably, the ^7Li NMR signal of $1Li[B(C_6F_5)_4]$ (δ = −6.7 ppm) appears in the common range of π-complexated Li^{+} ions,[55] but at considerably higher field than that of $[Li(Et_2O)_{2.5}][B(C_6F_5)_4]$ (δ = −1.1 ppm in C_6H_5F). This observation suggests a tight encapsulation of the Li^{+} ion by **1** in solution.

The ^1H and ^{13}C NMR spectra of $1M[BAr_4]$ display a single set of signals for the two Idipp substituents indicating that a rapid site exchange of the η^6-coordinated dipp groups with those which are not bonded to the alkali metal ions occurs on

the NMR time scale (see SI, Figures S23−S25 and S27−S29). No splitting of the ^1H NMR signals was observed at −40 °C just above the freezing point of C_6D_5Cl (−45 °C). It is presently unclear whether this site exchange is an intramolecular process involving a successive or concomitant rotation of the NHC groups about the respective Si−C_{NHC} bonds. An intermolecular Li^{+} exchange seems less probable given the broadening of the ^{29}Si NMR resonance induced by the unresolved spin−spin coupling.

Quantum chemical calculations of the cation $1Li^{+}$ were carried out on the B97-D3/**I** level of theory to analyze the interaction of Li^{+} with the (Idipp)Si=Si(Idipp) core of **1**.[43] The structural parameters of the optimized minimum structure $1Li^{+}_{calc}$ agree well with the experimental values (see SI, Table S6).

A look at the Kohn−Sham orbitals of $1Li^{+}_{calc}$ revealed the same sequence of frontier orbitals as in **1**, in which the $n_+(Si−Si)$ orbital is the HOMO, the Si=Si π-orbital is the HOMO−1 and the $n_-(Si−Si)$ orbital is the HOMO−2 (see SI, Figure S43).[8,18] No orbitals pointing to an interaction between Li^{+} and the η^2-coordinated Si=Si bond or the η^6-coordinated aryl substituents were found by the calculations due to the mainly electrostatic bonding of Li^{+}, which was further confirmed by an NBO analysis of $1Li^{+}_{calc}$ (see SI, Table S12). The Li atom displays a lone vacancy with a small occupancy of 0.13. Second order perturbation theory analysis of the Fock matrix in the NBO basis revealed only small interaction energies between the Si-based or aryl-based donor NBOs and the lone vacancy on the Li atom (see SI, Table S13), which is characteristic of electrostatic cation−π interactions.[56]

Consequently, the encapsulation of the Li^{+} cation in the cavity of **1** is accompanied by only a minor charge transfer to the Li^{+} ion, which still carries a high positive charge in $1Li^{+}_{calc}$ according to an NPA charge analysis ($q(Li)$ = 0.85e). This charge transfer occurs exclusively from the NHCs, as evidenced by the essentially identical NPA charges of the Si atoms in $1Li^{+}$ ($q(Si1)$ = −0.12e, $q(Si2)$ = −0.11e) and in **1** ($q(Si1,Si2)$ = −0.10e) (see SI, Tables S7 and S12).

2.5. Quantum Chemical Calculations of a Series of Isolobal Compounds with $[(Idipp)(R)Si^{II}{=}Si^{0}(Idipp)]^{+}$. Formal replacement of the [Si(Idipp)] fragments in $[(Idipp)-(R)Si^{II}{=}Si^{0}(Idipp)]^{+}$ ($1R^{+}$, R = H, Me, Et) by the isolobal fragments $[SiR]^{-}$ and $[PR]$[19,20] leads to a series of Si and P multiple-bonded compounds **B−F**, which are depicted in Scheme 5. Class **B**,[12] **C**[27] and **F**[23a] compounds are very rare, whereas disilenide anions (**D**)[28,48,57] and phosphasilenes (**E**)[58] are familiar classes of compounds, the synthetic potential of which has been exploited. A comparison of **A** with **B−F** unraveled many common structural features, which stimulated us to study their electronic structures.

For this purpose quantum chemical calculations of the model systems with NHC^{Me} = $C[N(Me)CH]_2$ and R = Me were carried out on the B97-D3/RI-JCOSX/def2-TZVP level of theory.[43] The optimized minimum structures are depicted in Figure 7 and selected bonding parameters are given in Table 3.
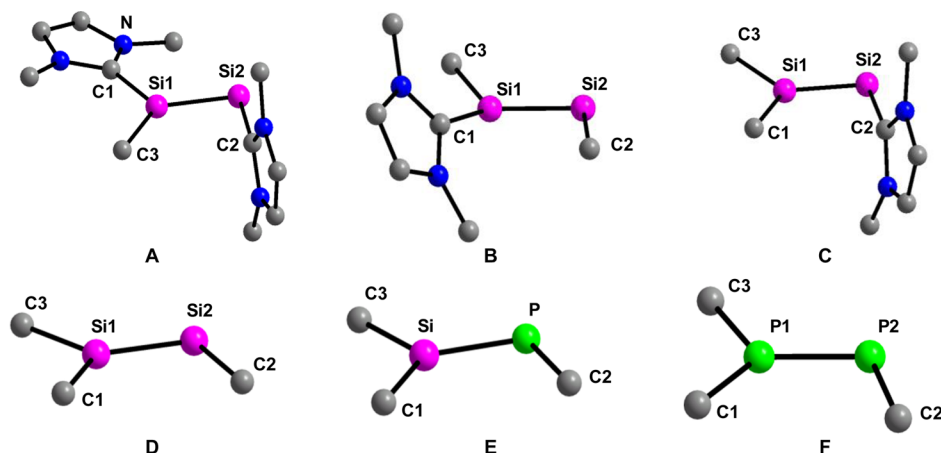
Figure 7. Calculated minimum structures of the model compounds **A**–**F** (NHC^{Me} = C[N(Me)CH]$_2$, R = Me) depicted in Scheme 5. Hydrogen atoms were omitted for simplicity reasons.

Table 3. Selected Calculated Bond Lengths, Bond Angles and Dihedral Angles of Compounds A–F Depicted in Figure 7[a]

	E1–E2 [Å]	E1–C1 [Å]	E2–C2 [Å]	E1–C3 [Å]	C1–E1–E2 [deg]	C2–E2–E1 [deg]
A	2.213	1.890	1.946	1.900	118.45	89.50
B	2.240	1.882	1.962	1.911	121.59	101.14
C	2.192	1.910	1.931	1.900	129.55	88.91
D	2.210	1.935	1.997	1.927	132.00	99.53
E	2.083[d]	1.885[d]	1.889[d]	1.881[d]	129.14[d]	102.08[d]
F	2.010	1.812	1.850	1.807	130.06	104.02

	C1–E1–C3 [deg]	C3–E1–E2 [deg]	Σ(E1)[b] [deg]	φ_{NHC1}[c] [deg]	φ_{NHC2}[c] [deg]
A	111.66	129.85	359.96	12.79	91.96
B	109.06	124.43	355.08	53.23	–
C	108.23	122.18	359.96	–	96.26
D	104.95	123.05	360.00	–	–
E	111.76[d]	119.76[d]	360.00[d]	–	–
F	112.80	117.14	360.00	–	–

[a]E = Si or P. [b]Σ(E1) is the sum of angles around the E1 atom. [c]φ_{NHC1} and φ_{NHC2} are the dihedral angles between the least-squares planes of the C1–E1–E2–C2 atoms and the heterocyclic ring atoms of the NHC substituents bonded to E1 and E2, respectively. [d]E1 = Si, E2 = P.

The structures of compounds **A**, **C**, **D**, **E** and **F** are quite similar as evidenced by the similar Si–Si, Si–C$_{NHC}$ and Si–C$_{methyl}$ bond lengths, the similar C1–E1–E2, C2–E2–E1, C1–E1–C3 and C3–E1–E2 bond angles (E = Si or P), the planar geometry around the E1 atoms and the orthogonal orientation of the Si2-bonded NHC substituent in compounds **A** and **C** with respect to the C1–Si1–Si2–C2 plane. The structural parameters of compound **B** differ slightly from those of compounds **A** and **C**, which becomes apparent from the slight pyramidalization of the Si1 atom and the synclinal orientation of the Si1-bonded NHC substituent toward the C1–Si1–Si2–C2 plane.

A look at the Kohn–Sham orbitals of compounds **A**–**F** reveals the same sequence of frontier orbitals as expected for isolobal compounds (Table 4). Thus, the HOMOs are in all cases the E≡E π-orbitals, the HOMOs−1 the lone pair orbitals at the two-coordinated E2 atoms (E2 = Si or P), and the LUMOs of compounds **A**, **B**, **D**, **E** and **F** the E≡E π*-orbitals. In the NHC-substituted compounds **A** and **B** a significant
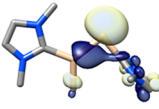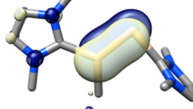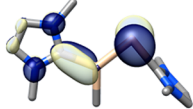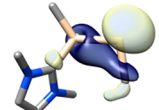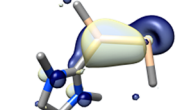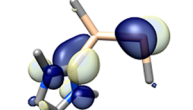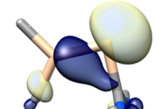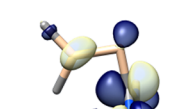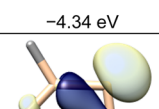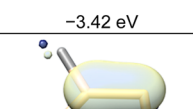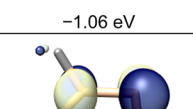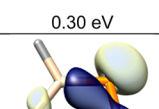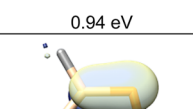
stabilization of the Si≡Si π*-orbital occurs via a bonding interaction with the C$_{NHC}$- and N$_{NHC}$-centered π*-orbital of the NHC^{Me}-substituent. In compound **C** the Si≡Si π*-orbital is the LUMO+1, whereas the LUMO is mainly the C$_{NHC}$- and N$_{NHC}$-centered π* orbital of the Si2-bonded NHC-substituent. It is noteworthy that the Kohn–Sham orbitals of **1H$^+_{calc}$**, **1Me$^+_{calc}$** (see SI, Figures S39 and S41), [(Idipp)(I)Si≡Si(Idipp)]$^+$,[4] Tbb(Br)Si≡Si(SIdipp)[12] and the model compound (IMe$_4$)(R)Si≡SiR (R = SiMe$_3$)[27] compare well those of the respective model systems depicted in Table 4.

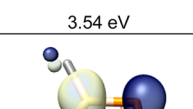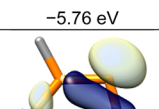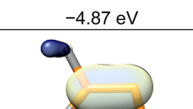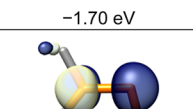Whereas compounds **A**–**F** reveal the same number, symmetry properties and the same occupation of the frontier orbitals with electrons, the absolute energies of the frontier orbitals of **A**–**F** differ significantly (Table 4). This is not surprising given the different charges of the compounds and the considerable higher electronegativity of the [PR] than that of the [Si(NHC)] or [SiR]$^−$ fragment, and implies a quite different reactivity of **A**–**F**, which remains to be exploited for the silicon compounds **A**–**C**. The interrelationship of **A**–**F** provides a different view of the bonding between NHCs and main-group elements from that developed by G. Frenking,[14] and enables one to conceive many presently unknown Si compounds that are related to known phosphorus congeners.

3. SUMMARY

The mixed-valent disilicon(I) borates **1R**[B(Ar^F)$_4$] (R = H, Me, Et) were obtained upon electrophilic addition of R$^+$ to **1** and were comprehensively analyzed by a combination of structural, spectroscopic and quantum chemical methods. The unprecedented 1,2-hydrogen migration observed along the Si≡Si bond of **1H**[B(Ar^F)$_4$] is reminiscent of the degenerate isomerization of carbenium ions, and can be considered as a molecular model for the H-migration in hydrogenated amorphous silicon that is of relevance in photovoltaics. The cations **1R$^+$** have considerable synthetic potential in silicon chemistry given their many potential reactivity sites, and can be strikingly viewed as NHC-trapped examples of the cations [Si$_2$R]$^+$, providing another example for the exceptional ability of NHCs to stabilize low-valent silicon centers in unusual bonding environments. The interrelation of the electronic structure of the cations **1R$^+$** to those of a series of Si and P multiple-bonded compounds that are obtained upon replacement of the [Si(NHC)] by the isolobal [PR] and [SiR]$^−$ fragments provides a different view on the electronic structure of NHC-stabilized

Table 4. Selected Kohn−Sham Orbitals and Their Energy Eigenvalues of Compounds A−F depicted in Figure 7[a]

	HOMO−1	HOMO	LUMO
$[(NHC^{Me})(R)Si=Si(NHC^{Me})]^+$ (**A**)			
	−7.89 eV	−7.23 eV	−5.26 eV
$(NHC^{Me})(R)Si=SiR$ (**B**)			
	−3.95 eV	−3.50 eV	−1.73 eV
$R_2Si=Si(NHC^{Me})$ (**C**)			
	−4.34 eV	−3.42 eV	−1.06 eV
$[R_2Si=SiR]^-$ (**D**)			
	0.30 eV	0.94 eV	3.54 eV
$R_2Si=PR$ (**E**)			
	−5.76 eV	−4.87 eV	−1.70 eV
$[R_2P=PR]^+$ (**F**)			
	−11.82 eV	−11.30 eV	−8.07 eV

[a]$NHC^{Me} = C[N(Me)CH]_2$, R = Me. Isosurface value: 0.05 e Bohr^{-3}.

main-group element compounds. The Si^0 compound **1** bears an optimal cavity for the complexation of alkali metal cations as demonstrated by the isolation and full characterization of **1M**[BAr$_4$] (M = Li, Na), which may become valuable reagents for the functionalization of **1** in reactions with main-group element or transition-metal halides.

ASSOCIATED CONTENT

ⓈSupporting Information

The Supporting Information is available free of charge on the ACS Publications website at DOI: 10.1021/jacs.6b01018.

Crystallographic data for **1H**[B(Ar^F)$_4$], **1Me**[B(Ar^F)$_4$], **1Et**[B(Ar^F)$_4$], **1Li**[B(C$_6$F$_5$)$_4$]·(n-C$_6$H$_{14}$) and **1Na**[B-(Ar^F)$_4$] (also deposited with the Cambridge Structural Database under the deposition numbers CCDC 1448827−1448831). (CIF)

Syntheses, analytical data and illustrations of the ^{1}H, ^{13}C{^{1}H} and ^{29}Si{^{1}H} NMR spectra of **1H**[B(Ar^F)$_4$], **1Me**[B(Ar^F)$_4$], **1Et**[B(Ar^F)$_4$], **1Li**[B(C$_6$F$_5$)$_4$], and **1Na**[B(Ar^F)$_4$]. Analysis of the dynamic process of **1H**[B(Ar^F)$_4$] in solution as well as details of the quantum chemical calculations. (PDF)

AUTHOR INFORMATION

Corresponding Author

*filippou@uni-bonn.de

Notes

The authors declare no competing financial interest.

ACKNOWLEDGMENTS

REFERENCES

(1) For recent reviews, see: (a) Wang, Y.; Robinson, G. H. *Chem. Commun.* **2009**, 5201. (b) Wang, Y.; Robinson, G. H. *Dalton Trans.* **2012**, *41*, 337. (c) Roesky, H. W. *J. Organomet. Chem.* **2013**, *730*, 57. (d) Ghadwal, R. S.; Azhakar, R.; Roesky, H. W. *Acc. Chem. Res.* **2013**, *46*, 444. (e) Wilson, D. J. D.; Dutton, J. L. *Chem. - Eur. J.* **2013**, *19*, 13626. (f) Martin, C. D.; Soleilhavoup, M.; Bertrand, G. *Chem. Sci.* **2013**, *4*, 3020. (g) Wang, Y.; Robinson, G. H. *Inorg. Chem.* **2014**, *53*, 11815. (h) Rivard, E. *Struct. Bonding (Berlin, Ger.)* **2013**, *156*, 203.

(2) Wang, Y.; Xie, Y.; Wei, P.; King, R. B.; Schaefer, H. F., III; Schleyer, P. v. R.; Robinson, G. H. *Science* **2008**, *321*, 1069.

(3) Xiong, Y.; Yao, S.; Inoue, S.; Epping, J. D.; Driess, M. *Angew. Chem., Int. Ed.* **2013**, *52*, 7147; *Angew. Chem.* **2013**, *125*, 7287.

(4) Arz, M. I.; Geiß, D.; Straßmann, M.; Schnakenburg, G.; Filippou, A. C. *Chem. Sci.* **2015**, *6*, 6515.

(5) (a) Ghadwal, R. S.; Roesky, H. W.; Merkel, S.; Henn, J.; Stalke, D. *Angew. Chem., Int. Ed.* **2009**, *48*, 5683; *Angew. Chem.* **2009**, *121*, 5793. (b) Filippou, A. C.; Chernov, O.; Schnakenburg, G. *Angew. Chem., Int. Ed.* **2009**, *48*, 5687; *Angew. Chem.* **2009**, *121*, 5797. (c) Filippou, A. C.; Chernov, O.; Schnakenburg, G. *Chem. - Eur. J.* **2011**, *17*, 13574. (d) Filippou, A. C.; Lebedev, Y. N.; Chernov, O.; Straßmann, M.; Schnakenburg, G. *Angew. Chem., Int. Ed.* **2013**, *52*, 6974; *Angew. Chem.* **2013**, *125*, 7112.

(6) (a) Filippou, A. C.; Chernov, O.; Blom, B.; Stumpf, K. W.; Schnakenburg, G. *Chem. - Eur. J.* **2010**, *16*, 2866. (b) Cui, H.; Cui, C. *Dalton Trans.* **2011**, *40*, 11937. (c) Al-Rafia, S. M. I.; McDonald, R.; Ferguson, M. J.; Rivard, E. *Chem. - Eur. J.* **2012**, *18*, 13810. (d) Inoue, S.; Eisenhut, C. *J. Am. Chem. Soc.* **2013**, *135*, 18315. (e) Agou, T.; Hayakawa, N.; Sasamori, T.; Matsuo, T.; Hashizume, D.; Tokitoh, N. *Chem. - Eur. J.* **2014**, *20*, 9246.

(7) Cowley, M. J.; Huch, V.; Rzepa, H. S.; Scheschkewitz, D. *Nat. Chem.* **2013**, *5*, 876.

(8) Arz, M. I.; Straßmann, M.; Meyer, A.; Schnakenburg, G.; Schiemann, O.; Filippou, A. C. *Chem. - Eur. J.* **2015**, *21*, 12509.

(9) Ahmad, S. U.; Szilvási, T.; Inoue, S. *Chem. Commun.* **2014**, *50*, 12619.

(10) (a) Jana, A.; Huch, V.; Scheschkewitz, D. *Angew. Chem., Int. Ed.* **2013**, *52*, 12179; *Angew. Chem.* **2013**, *125*, 12401. (b) Jana, A.; Majumdar, M.; Huch, V.; Zimmer, M.; Scheschkewitz, D. *Dalton Trans.* **2014**, *43*, 5175.

(11) Geiß, D.; Arz, M. I.; Straßmann, M.; Schnakenburg, G.; Filippou, A. C. *Angew. Chem., Int. Ed.* **2015**, *54*, 2739; *Angew. Chem.* **2015**, *127*, 2777.

(12) Ghana, P.; Arz, M. I.; Das, U.; Schnakenburg, G.; Filippou, A. C. *Angew. Chem., Int. Ed.* **2015**, *54*, 9980; *Angew. Chem.* **2015**, *127*, 10118.

(13) (a) Himmel, D.; Krossing, I.; Schnepf, A. *Angew. Chem., Int. Ed.* **2014**, *53*, 370; *Angew. Chem.* **2014**, *126*, 378. (b) Frenking, G. *Angew. Chem., Int. Ed.* **2014**, *53*, 6040; *Angew. Chem.* **2014**, *126*, 6152. (c) Himmel, D.; Krossing, I.; Schnepf, A. *Angew. Chem., Int. Ed.* **2014**, *53*, 6047; *Angew. Chem.* **2014**, *126*, 6159. (d) Köppe, R.; Schnöckel, H. *Chem. Sci.* **2015**, *6*, 1199. (e) Perras, F. A.; Ewing, C. A.; Dellermann, T.; Böhnke, J.; Ullrich, S.; Schäfer, T.; Braunschweig, H.; Bryce, D. L. *Chem. Sci.* **2015**, *6*, 3378.

(14) (a) Frenking, G.; Tonner, R. In *The Chemical Bond—Chemical Bonding Across the Periodic Table*; Frenking, G., Shaik, S., Eds.; Wiley-VCH: Weinheim, 2014; Chapter 4, pp 71−112. (b) Holzmann, N.; Andrada, D. M.; Frenking, G. *J. Organomet. Chem.* **2015**, *792*, 139.

(15) (a) Dyker, C. A.; Bertrand, G. *Science* **2008**, *321*, 1050. (b) Sidiropoulos, A.; Jones, C.; Stasch, A.; Klein, S.; Frenking, G. *Angew. Chem., Int. Ed.* **2009**, *48*, 9701; *Angew. Chem.* **2009**, *121*, 9881. (c) Jones, C.; Sidiropoulos, A.; Holzmann, N.; Frenking, G.; Stasch, A. *Chem. Commun.* **2012**, *48*, 9855. (d) Frenking, G.; Holzmann, N. *Science* **2012**, *336*, 1394. (e) Holzmann, N.; Dange, D.; Jones, C.; Frenking, G. *Angew. Chem., Int. Ed.* **2013**, *52*, 3004; *Angew. Chem.* **2013**, *125*, 3078.

(16) (a) Bruna, P. J.; Peyerimhoff, S. D.; Buenker, R. J. *J. Chem. Phys.* **1980**, *72*, 5437. (b) Peyerimhoff, S. D.; Buenker, R. J. *Chem. Phys.* **1982**, *72*, 111.

(17) The B3LYP/6-311+G**/6-31G* computed ZPVE corrected (ZPVE = zero point vibrational energy) dissociation energies for the stepwise dissociation of the carbene substituents from $Si_2(Idipp)_2$ at 0 K amount to 126.5 kJ mol^{-1} ($Si_2(Idipp)_2 \rightarrow Si_2(Idipp)$ ($S = 0$) + Idipp ($S = 0$)) and 185.0 kJ mol^{-1} ($Si_2(Idipp) \rightarrow Si_2$ ($S = 1$, $X^3\Sigma_g^-$) + Idipp ($S = 0$)) (S is the total spin angular momentum of the electronically and geometrically relaxed fragments), see ref 8.

(18) For a quantum chemical description of through-bond and through-space interactions leading to n$_+$ and n$_-$ lone pair orbitals see: (a) Hoffmann, R. *Acc. Chem. Res.* **1971**, *4*, 1. (b) Albright, T. A.; Burdett, J. K.; Whangbo, M.-H. *Orbital Interactions in Chemistry*, 2nd ed.; Wiley-Interscience: Hoboken, NJ, 2013; Chapter 11, pp 241−271.

(19) Nobel lecture on isolobal analogy: Hoffmann, R. *Angew. Chem., Int. Ed. Engl.* **1982**, *21*, 711; *Angew. Chem.* **1982**, *94*, 725.

(20) In an approach for the formal classification of covalent compounds of transition metals, a neutral 2e-donor as Idipp has been also considered as equivalent to R$^-$ (R = alkyl, aryl): Green, M. L. H. *J. Organomet. Chem.* **1995**, *500*, 127.

(21) (a) Cowley, A. H.; Norman, N. C.; Pakulski, M. *J. Chem. Soc., Chem. Commun.* **1984**, 1054. (b) Cowley, A. H.; Kilduff, J. E.; Norman, N. C.; Pakulski, M. *J. Chem. Soc., Dalton Trans.* **1986**, 1801. (c) Partyka, D. V.; Washington, M. P.; Gray, T. G.; Updegraff, J. B., III; Turner, J. F., II; Protasiewicz, J. D. *J. Am. Chem. Soc.* **2009**, *131*, 10041.

(22) (a) Chen, M.; Wang, Y.; Xie, Y.; Wei, P.; Gilliard, R. J., Jr.; Schwartz, N. A.; Schaefer, H. F., III; Schleyer, P. v. R.; Robinson, G. H. *Chem. - Eur. J.* **2014**, *20*, 9208. (b) Arz, M. I. Molecular Si(0) and Si(I) Compounds: Synthesis, Structure and Reactivity. Ph.D. Thesis, University of Bonn, 2016. (c) Arz, M. I.; Schnakenburg, G.; Filippou, A. C. n and π Complexes of NHC-stabilized Disilicon(0). *Proceedings of the 14th International Symposium on Inorganic Ring Systems*, Regensburg, July 26−31, 2015. (d) Arz, M. I.; Straßmann, M.; Schnakenburg, G.; Filippou, A. C. Chemistry of NHC-stabilized Disilicon(0). *Proceedings of the 46th Silicon Symposium*, Davis, CA, June 21−24, 2015.

(23) (a) Loss, S.; Widauer, C.; Grützmacher, H. *Angew. Chem., Int. Ed.* **1999**, *38*, 3329; *Angew. Chem.* **1999**, *111*, 3546. (b) Cowley, A. H.; Kilduff, J. E.; Norman, N. C.; Pakulski, M. *J. Am. Chem. Soc.* **1983**, *105*, 4845.

(24) (a) Brookhart, M.; Grant, B.; Volpe, A. F., Jr. *Organometallics* **1992**, *11*, 3920. (b) Taube, R.; Wache, S. *J. Organomet. Chem.* **1992**, *428*, 431.

(25) Batsanov, S. S. *Inorg. Mater.* **2001**, *37*, 871.

(26) φ_{NHC1} and φ_{NHC2} denotes the dihedral angle between the C$_{NHC}$-Si-Si−C$_{NHC}$ least-squares plane and the least-squares plane of the N-heterocyclic ring bonded to the Si1 and Si2 atom, respectively.

(27) Yamaguchi, T.; Sekiguchi, A.; Driess, M. *J. Am. Chem. Soc.* **2010**, *132*, 14061.

(28) Kinjo, R.; Ichinohe, M.; Sekiguchi, A. *J. Am. Chem. Soc.* **2007**, *129*, 26.

(29) Chernov, O. Novel Molecular Si(II) Precursors for Synthesis of the First Compounds with Metal-Silicon Triple Bonds. Ph.D. Thesis, University of Bonn, 2012.

(30) Agou, T.; Sugiyama, Y.; Sasamori, T.; Sakai, H.; Furukawa, Y.; Takagi, N.; Guo, J.-D.; Nagase, S.; Hashizume, D.; Tokitoh, N. *J. Am. Chem. Soc.* **2012**, *134*, 4120.

(31) (a) Simons, R. S.; Haubrich, S. T.; Mork, B. V.; Niemeyer, M.; Power, P. P. *Main Group Chem.* **1998**, *2*, 275. (b) Weidemann, N.; Schnakenburg, G.; Filippou, A. C. *Z. Anorg. Allg. Chem.* **2009**, *635*, 253.

(32) Binsch, G.; Eliel, E. L.; Kessler, H. *Angew. Chem., Int. Ed. Engl.* **1971**, *10*, 570; *Angew. Chem.* **1971**, *83*, 618.

(33) Arduengo, A. J., III; Krafczyk, R.; Schmutzler, R.; Craig, H. A.; Goerlich, J. R.; Marshall, W. J.; Unverzagt, M. *Tetrahedron* **1999**, *55*, 14523.

(34) Iggo, J. A. *NMR Spectroscopy in Inorganic Chemistry*; Oxford University Press: Oxford, England, 1999.

(35) Dolgonos, G. *Chem. Phys. Lett.* **2008**, *466*, 11.

(36) Dürr, M.; Höfer, U. *Prog. Surf. Sci.* **2013**, *88*, 61.

(37) (a) Staebler, D. L.; Wronski, C. R. *Appl. Phys. Lett.* **1977**, *31*, 292. (b) Branz, H. M. *Phys. Rev. B: Condens. Matter Mater. Phys.* **1999**, *59*, 5498.

(38) (a) Haselbach, E.; Heilbronner, E. *Tetrahedron Lett.* **1967**, *8*, 4531. (b) Hoefnagel, M. A.; van Veen, A.; Wepster, B. M. *Rec. Trav. Chim. Pays-Bas* **1969**, *88*, 562. (c) Haselbach, E. *Helv. Chim. Acta* **1970**, *53*, 1526. (d) Eian, G. L.; Kingsbury, C. A. *Bull. Chem. Soc. Jpn.* **1970**, *43*, 739. (e) Cox, R. A.; Buncel, E. In *The Chemistry of the Hydrazo, Azo and Azoxy Groups*; Patai's Chemistry of Functional Groups; Patai, S., Ed.; Wiley-Interscience: New York, 1975; Vol. 2, Chapter 18, pp 775−859. (f) Kuroda, Y.; Lee, H.; Kuwae, A. *J. Phys. Chem.* **1980**, *84*, 3417.

(39) For selected reviews, see: (a) Leone, R. E.; Schleyer, P. v. R. *Angew. Chem., Int. Ed. Engl.* **1970**, *9*, 860; *Angew. Chem.* **1970**, *82*, 889. (b) Olah, G. A. *J. Am. Chem. Soc.* **1972**, *94*, 808. (c) Olah, G. A. *Angew. Chem., Int. Ed. Engl.* **1973**, *12*, 173; *Angew. Chem.* **1973**, *85*, 183. (d) McMurry, J. E.; Lectka, T. *Acc. Chem. Res.* **1992**, *25*, 47.

(40) Taking the equation $\Delta G^{\neq} = 0.01914 \cdot T \cdot [9.972 + \lg(T/\Delta\nu)]$, the smallest separation ($\Delta\nu$) of two signals of the heterotopic Idipp substituents in the ^{1}H NMR spectrum at 298 K ($\Delta\nu$ = 7.6 Hz) and the boiling point of THF-d_8 (T = 338 K), a low limit of the Gibbs energy of activation can be estimated to be $\Delta G^{\neq}$ = 75 kJ mol^{-1} (Sandström, D. *Dynamic NMR Spectroscopy*; Academic Press: London, 1992).

(41) (a) Hunter, B. K.; Reeves, L. W. *Can. J. Chem.* **1968**, *46*, 1399. (b) Schraml, J.; Chvalovský, V.; Mägi, M.; Lippmaa, E. *Collect. Czech. Chem. Commun.* **1979**, *44*, 854.

(42) Dorman, D. E.; Jautelat, M.; Roberts, J. D. *J. Org. Chem.* **1971**, *36*, 2757.

(43) ORCA 3.0.0 program package: (a) Neese, F. *WIREs Comput. Mol. Sci.* **2012**, *2*, 73. B97-D3 functional: (b) Grimme, S. *J. Comput. Chem.* **2006**, *27*, 1787. (c) Grimme, S.; Antony, J.; Ehrlich, S.; Krieg, H. *J. Chem. Phys.* **2010**, *132*, 154104. (d) Grimme, S.; Ehrlich, S.; Goerigk, L. *J. Comput. Chem.* **2011**, *32*, 1456. COSMO model: (e) Klamt, A.; Schüürmann, G. *J. Chem. Soc., Perkin Trans. 2* **1993**, 799. RI-JCOSX approximations: (f) Neese, F. *J. Comput. Chem.* **2003**, *24*, 1740. (g) Neese, F.; Wennmohs, F.; Hansen, A.; Becker, U. *Chem. Phys.* **2009**, *356*, 98. def2-TZVP and def2-SVP basis sets: (h) Schäfer, A.; Horn, H.; Ahlrichs, R. *J. Chem. Phys.* **1992**, *97*, 2571. (i) Weigend, F.; Ahlrichs, R. *Phys. Chem. Chem. Phys.* **2005**, *7*, 3297. NBO 6.0 program: (j) Glendening, E. D.; Badenhoop, J. K.; Reed, A. E.; Carpenter, J. E.; Bohmann, J. A.; Morales, C. M.; Landis, C. R.; Weinhold, F. *NBO 6.0*; Theoretical Chemistry Institute, University of Wisconsin, Madison, WI, 2013.

(44) The term "σ-bonded" isomer was used to indicate that this isomer features a Si–R σ-bond (R = H, Me, Et) resulting from the interaction of the n$_+$ lone pair orbital of **1** with the LUMO of the electrophile R$^+$ (R = H, Me, Et). In comparison, the "π-bonded" isomer features a 3c-2e bond resulting from the interaction of the Si=Si π bond of **1** with the LUMO of the electrophile.

(45) Holleman, A. F.; Wiberg, E. *Inorganic Chemistry*; Academic Press: San Diego, 2001; *Lehrbuch der Anorganischen Chemie*, 101. verbesserte und stark erweiterte Auflage, deGruyter: Berlin, 2001.

(46) (a) Massey, A. G.; Park, A. J. *J. Organomet. Chem.* **1964**, *2*, 245. (b) Lehmann, M.; Schulz, A.; Villinger, A. *Angew. Chem., Int. Ed.* **2009**, *48*, 7444; *Angew. Chem.* **2009**, *121*, 7580.

(47) (a) Nishida, H.; Takada, N.; Yoshimura, M.; Sonoda, T.; Kobayashi, H. *Bull. Chem. Soc. Jpn.* **1984**, *57*, 2600. (b) Bahr, S. R.; Boudjouk, P. *J. Org. Chem.* **1992**, *57*, 5545. (c) Reger, D. L.; Little, C. A.; Lamba, J. J. S.; Brown, K. J.; Krumper, J. R.; Bergman, R. G.; Irwin, M.; Fackler, J. P., Jr. *Inorg. Synth.* **2004**, *34*, 5. (d) Yakelis, N. A.; Bergman, R. G. *Organometallics* **2005**, *24*, 3579.

(48) Scheschkewitz, D. *Angew. Chem., Int. Ed.* **2004**, *43*, 2965; *Angew. Chem.* **2004**, *116*, 3025.

(49) Wiberg, N.; Amelunxen, K.; Lerner, H.-W.; Schuster, H.; Nöth, H.; Krossing, I.; Schmidt-Amelunxen, M.; Seifert, T. *J. Organomet. Chem.* **1997**, *542*, 1.

(50) For a review on cation–π interactions and their importance in biological systems and material science, see: Ma, J. C.; Dougherty, D. A. *Chem. Rev.* **1997**, *97*, 1303.

(51) King, B. T.; Noll, B. C.; Michl, J. *Collect. Czech. Chem. Commun.* **1999**, *64*, 1001.

(52) Bertermann, R.; Braunschweig, H.; Constantinidis, P.; Dellermann, T.; Dewhurst, R. D.; Ewing, W. C.; Fischer, I.; Kramer, T.; Mies, J.; Phukan, A. K.; Vargas, A. *Angew. Chem., Int. Ed.* **2015**, *54*, 13090; *Angew. Chem.* **2015**, *127*, 13282.

(53) (a) Kira, M.; Sekiguchi, Y.; Iwamoto, T.; Kabuto, C. *J. Am. Chem. Soc.* **2004**, *126*, 12778. (b) Fischer, R.; Zirngast, M.; Flock, M.; Baumgartner, J.; Marschner, C. *J. Am. Chem. Soc.* **2005**, *127*, 70. (c) Iwamoto, T.; Sekiguchi, Y.; Yoshida, N.; Kabuto, C.; Kira, M. *Dalton Trans.* **2006**, 177. (d) Hartmann, M.; Haji-Abdi, A.; Abersfelder, K.; Haycock, P. R.; White, A. J. P.; Scheschkewitz, D.

Dalton Trans. **2010**, *39*, 9288. (e) Abe, T.; Iwamoto, T.; Kira, M. *J. Am. Chem. Soc.* **2010**, *132*, 5008.

(54) Selected references: (a) Edlund, U.; Lejon, T.; Venkatachalam, T. K.; Buncel, E. *J. Am. Chem. Soc.* **1985**, *107*, 6408. (b) Becker, G.; Hartmann, H.-M.; Hengge, E.; Schrank, F. *Z. Anorg. Allg. Chem.* **1989**, *572*, 63. (c) Belzner, J.; Dehnert, U.; Stalke, D. *Angew. Chem., Int. Ed. Engl.* **1995**, *33*, 2450; *Angew. Chem.* **1994**, *106*, 2580. (d) Koizumi, T.; Morihashi, K.; Kikuchi, O. *Organometallics* **1995**, *14*, 4018. (e) Lee, V. Y.; Sekiguchi, A. *Organometallic Compounds of Low-Coordinate Si, Ge, Sn and Pb: From Phantom Species to Stable Compounds*; John Wiley & Sons: Chichster, West Sussex, U.K., 2010; Chapter 3, pp 89–138. (f) Däschlein, C.; Strohmann, C. *Eur. J. Inorg. Chem.* **2009**, *2009*, 43.

(55) The ^{7}Li NMR resonances of π-complexated Li atoms exhibit diagnostic upfield shifts, which result from the interaction with the aromatic ring current, see: (a) Elschenbroich, C.; Salzer, A. *Organometallics. A Concise Introduction*, 2nd ed.; VCH: Weinheim, Germany, 1992. (b) Johnels, D.; Günther, H. In *The Chemistry of Organolithium Compounds, Part 1*; Rappoport, Z., Marek, I., Eds.; John Wiley & Sons Ltd.: West Sussex, U.K., 2004; Chapter 4, pp 137–204.

(56) Mohajeri, A.; Karimi, E. *J. Mol. Struct.: THEOCHEM* **2006**, *774*, 71.

(57) (a) Ichinohe, M.; Sanuki, K.; Inoue, S.; Sekiguchi, A. *Organometallics* **2004**, *23*, 3088. (b) Inoue, S.; Ichinohe, M.; Sekiguchi, A. *Chem. Lett.* **2005**, *34*, 1564. (c) Iwamoto, T.; Kobayashi, M.; Uchiyama, K.; Sasaki, S.; Nagendran, S.; Isobe, H.; Kira, M. *J. Am. Chem. Soc.* **2009**, *131*, 3156. (d) Cowley, M. J.; Abersfelder, K.; White, A. J. P.; Majumdar, M.; Scheschkewitz, D. *Chem. Commun.* **2012**, *48*, 6595. Review articles: (e) Scheschkewitz, D. *Chem. - Eur. J.* **2009**, *15*, 2476. (f) Scheschkewitz, D. *Chem. Lett.* **2011**, *40*, 2.

(58) Selected references: (a) Smit, C. N.; Lock, F. M.; Bickelhaupt, F. *Tetrahedron Lett.* **1984**, *25*, 3011. (b) Smit, C. N.; Bickelhaupt, F. *Organometallics* **1987**, *6*, 1156. (c) Bender, H. R. G.; Niecke, E.; Nieger, M. *J. Am. Chem. Soc.* **1993**, *115*, 3314. (d) Driess, M. *Coord. Chem. Rev.* **1995**, *145*, 1. (e) Driess, M.; Block, S.; Brym, M.; Gamer, M. T. *Angew. Chem., Int. Ed.* **2006**, *45*, 2293; *Angew. Chem.* **2006**, *118*, 2351. (f) Yao, S.; Block, M.; Brym, M.; Driess, M. *Chem. Commun.* **2007**, 3844. (g) Lee, V. Y.; Kawai, M.; Sekiguchi, A.; Ranaivonjatovo, H.; Escudié, J. *Organometallics* **2009**, *28*, 4262. (h) Li, B.; Matsuo, T.; Hashizume, D.; Fueno, H.; Tanaka, K.; Tamao, K. *J. Am. Chem. Soc.* **2009**, *131*, 13222. (i) Hansen, K.; Szilvási, T.; Blom, B.; Inoue, S.; Epping, J.; Driess, M. *J. Am. Chem. Soc.* **2013**, *135*, 11795. (j) Willmes, P.; Cowley, M. J.; Hartmann, M.; Zimmer, M.; Huch, V.; Scheschkewitz, D. *Angew. Chem., Int. Ed.* **2014**, *53*, 2216; *Angew. Chem.* **2014**, *126*, 2248. (k) Breit, N. C.; Szilvási, T.; Inoue, S. *Chem. - Eur. J.* **2014**, *20*, 9312.